Effect of Forebody Strakes on Missile Asymmetric Vortices

Chih-Chung Yuan* and Richard M. Howard†
Naval Postgraduate School, Monterey, California 93943

Wind-tunnel tests were conducted on a 1/7th-scale vertically launched surface-to-air missile model to investigate the effects of forebody strakes on the side forces and yawing moments induced by nose-generated asymmetric vortices at high angles of attack. Test angles of attack ranged from 0 to 90 deg at a Reynolds number of 1.15×10^5, based on the model diameter, and at a Mach number of 0.11. The four-strake forebody demonstrated dramatic results in the elimination of yawing moments at high angles of attack. The eight-strake forebody showed mixed results, with three different responses over the angle-of-attack range from 45 to 75 deg. This configuration first caused a reduction in induced yawing moment, then a violent switching, and then at very high angles had no effect. Observations concerning the onset angles of forebody- and afterbody-generated asymmetric vortices indicate that an analysis of side forces alone is insufficient to consider possible control problems for a realistically configured missile.

Nomenclature

C_n = yawing moment coefficient, $= n/(\rho U_\infty^2/2)S(d)$
C_Y = side force coefficient, $= Y/(\rho U_\infty^2/2)S$
d = model body diameter, in.
l = model length, in.
M = Mach number
n = yawing moment, in./lb
Re = Reynolds number, $= \rho U_\infty d/\mu$
S = reference area, $= \pi d^2/4$, in.^{2}
U_∞ = freestream velocity, ft/s
Y = side force, lb
α = angle of attack, deg
μ = coefficient of molecular viscosity, slug/ft-h
ρ = air density, slug/ft^3
θ = roll angle, deg

Introduction

THE recent deployment of the Vertical Launch System (VLS) on board ships carrying surface-to-air (SAM) missiles represents a major advancement in Naval weapon system technology.[1] But a characteristic of vertically launched missiles is their inability to point at the target intercept point before launch. Since the missile cannot rely on the fire-control radar beam to guide it into its initial intercept trajectory, the missile must be maneuvered to this flight path. Requirements during the search and acquisition phase of the flight can place angle-of-attack demands on the missile up to 50 deg during pushover maneuvers.[2]

The existence of induced side forces and yawing moments on slender bodies due to the formation of asymmetric vortices at high angles of attack has been characterized by numerous investigators.[3-5] Unpredictable side forces may be generated under certain flow conditions for a vertically launched missile, posing a potential threat to flight stability. In 1987 a flight test was performed on the Vertical Launch ASROC (VLA) antisubmarine weapon. This missile is required to perform a hard pushover involving angles of attack up to 70 deg. During the pushover maneuver, control of the missile was lost due to yawing moments 150% greater than measured in wind-tunnel tests. A short time before departure, the nose cap tip became unseated; about 0.25 s later the tip reseated itself, but the yawing moment continued and control could not be regained. The incident was attributed to asymmetric vortex shedding.[6]

One viewpoint of previous work concerning the formation of asymmetric vortices at high angles of attack is that the phenomenon is extremely Reynolds-number dependent; the generation of strong side forces may occur where the body experiences subcritical (laminar) vortex separation on one side and critical separation on the other.[3] Other recent work supports the proposition that the principal cause of vortex asymmetry is a hydrodynamic instability of the inviscid flowfield.[4] The vortices, increasing in strength with angle of attack and crowding together for a sufficiently large value of nose fineness ratio, apparently interact with the surrounding potential flowfield to stabilize in a steady or quasisteady asymmetric configuration. This hypothesis is supported by flow visualization indicating that large asymmetries in the surface flow patterns existed when laminar separation occurred over the length of slender forebodies. Tests conducted over a range of Reynolds numbers suggest that the hydrodynamic instability is the stronger mechanism for producing side forces, with the second mechanism in the transitional separation regime being fairly weak.[7,8]

Various forebody modifications have been tested in an attempt to reduce or eliminate the induced side forces. These changes include nose blunting and the addition of strakes, helical trips, and surface perturbations. The effects of forebody modifications indicate the changes may be nonlinear; for example, nose blunting may reduce the side force but may trade a nose-generated vortex asymmetry for an afterbody-generated one. The first asymmetric vortex pair forming may be a strong pair generated by the afterbody, leading again to a large side force.[3]

The addition of strakes as a forebody modification has produced results that are not always consistent and may be configuration dependent. Reference 6 describes a series of tests for the addition of 16 strakes to the nose tip of the Vertical Launch ASROC mentioned previously. Induced yawing moments were cut in half in the high angle-of-attack range, but below 45 deg the moments were increased over the baseline values. For a slightly different configuration, with longer strakes, the yawing moments were generally reduced but increased rapidly beyond 70-deg angle of attack.

Received Sept. 26, 1990; revision received Feb. 15, 1991; accepted for publication Feb. 15, 1991; to be presented as Paper 91-2864 at the AIAA Atmospheric Flight Mechanics Conference, New Orleans, LA, Aug. 12-14, 1991.

*Graduate Student, Aeronautical Engineering Curriculum; currently, Chief Missile Officer, Taiwan, Republic of China Navy.

†Assistant Professor, Department of Aeronautics and Astronautics. Senior Member AIAA.

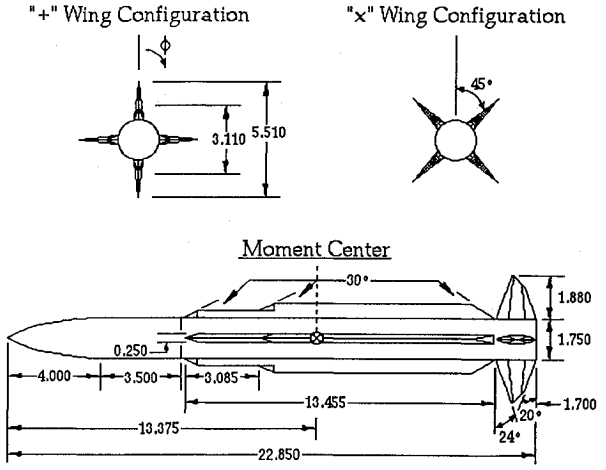

Fig. 1 VLSAM model (dimensions in inches).

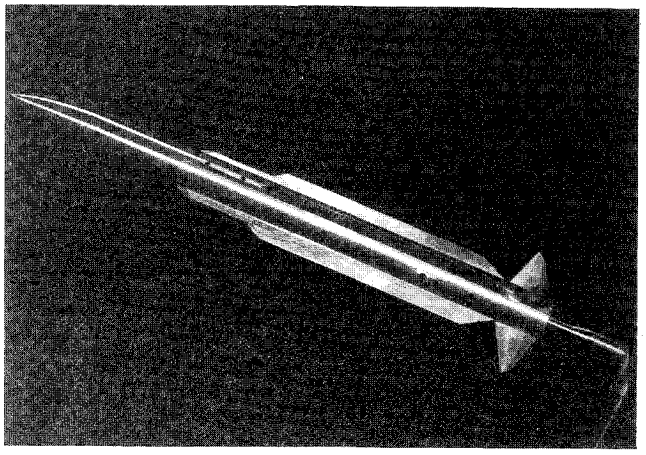

Fig. 2 VLSAM model.

The purpose of this paper is to study the effect of forebody strakes on the generation of asymmetric vortices for a ship-launched missile. Induced side forces and yawing moments were measured for two wing-body and three forebody-strake configurations (no-strake, four-strake, and eight-strake). Besides the motivation to determine a simple geometric modification for avoiding possible missile control problems at high angles of attack, the work was driven by the desire to gain a better understanding of the formation mechanism of the asymmetric vortices for a realistically configured missile.

Experimental Program

A wind-tunnel study of the induced side forces and yawing moments over angles of attack up to 90 deg was performed for a vertically launched surface-to-air missile (VLSAM) with and without forebody strakes. Body configurations compared were body-wings-tail at 0-deg roll angle (wings-tail in a "+" orientation), and body-wings-tail at 45-deg roll angle (wings-tail in an "x" orientation), as can be seen in Fig. 1. Because of the unsteady nature of the vortical flowfield, in order to resolve an accurate response to the modifications, measurements were recorded at 1-deg increments.

Model

The VLSAM is representative of current ship-based vertically launched surface-to-air missiles. The model is of a cruciform tail-control missile with narrow strakes and long strake-like dorsal wings. The model diameter is 1.75 in., the length is 22.85 in., and the ogive length-to-diameter ratio is 2.29; the model represents approximately a 1/7-scale missile. For minimum tunnel interference, the support system was constructed to pivot the model at its approximate center for angle-of-attack changes. The VLSAM was pitched in the horizontal plane. A sketch of the model is shown in Fig. 1, and a photograph of the model is shown in Fig. 2. It should be noted that a new forebody was machined for these tests, which is not the same forebody used in the experiments in Ref. 9.

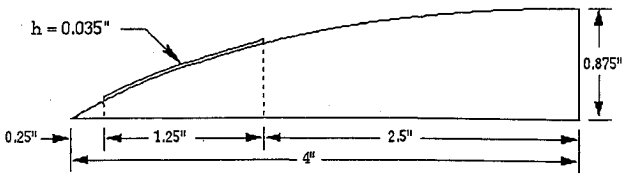

Fig. 3a Strake geometry on ogive forebody.

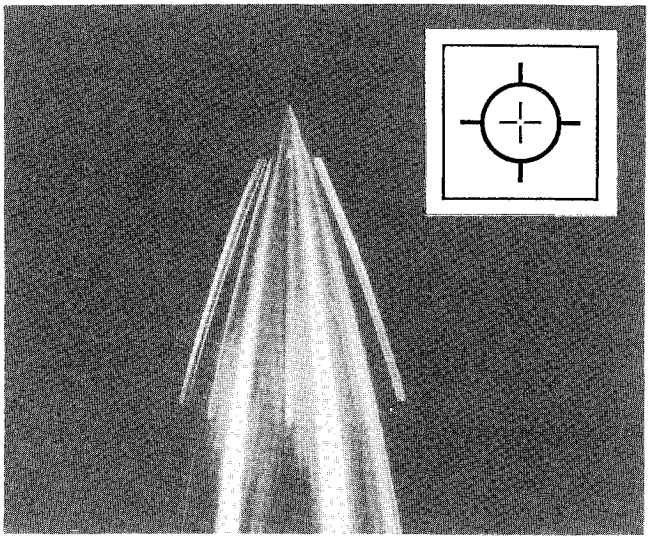

Fig. 3b Four-strake forebody (with + afterbody).

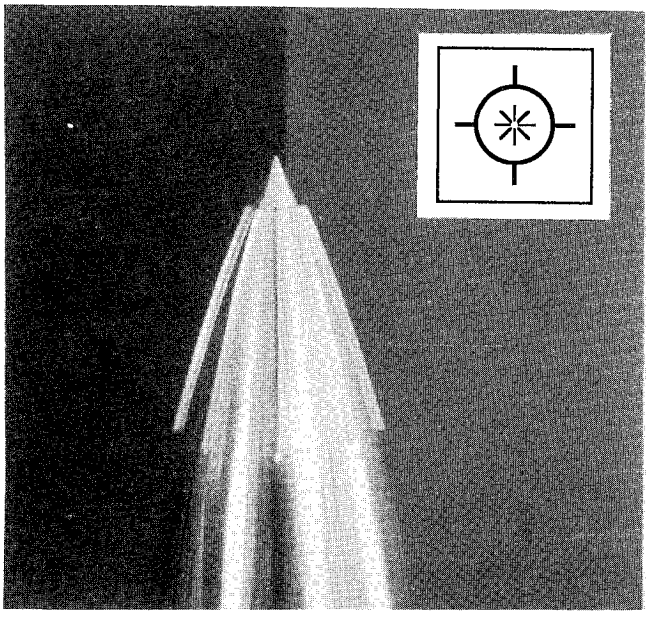

Fig. 3c Eight-strake forebody (with + afterbody).

Forces and moments were measured by an internal sting-mounted six-component strain-gauge balance. Force and moment data were corrected for solid blockage, but no correction was made for sting interference effects. Tail control surfaces were fixed. Side force coefficients were referred to an area based on the body diameter, and the diameter was used as an additional length scale for nondimensionalizing the yawing moments. The moment reference center was at a distance of 0.586 the length of the body measured from the nose. The six-component balance was calibrated at the NASA Ames Research Center before use at the Naval Postgraduate School;

check calibrations were performed with the balance in place in the wind tunnel.

Forebody Strakes

The strakes were designed with the intent of fixing the flow separation location along the forebody. The strake curvature followed the ogive nose at a height of $0.020d$. The strake thickness was $0.0143d$, and the length was $0.714d$. A sketch of one strake and its location are shown in Fig. 3a.

The forebody strakes were attached in two configurations, as shown in Figs. 3b and 3c. The four-strake forebody had the strakes arranged in a + orientation. The eight-strake forebody consisted of the four-strake nose with four additional strakes located symmetrically around the circumference. For strake installation, slots were machined in the aluminum forebody, and the strakes were attached with epoxy. Since a single nose roll angle was held during the experiments, a decision had to be made about which orientation, + or x, would be used for the four-strake case. The x orientation, therefore, could not be tested in the four-strake configuration without restoration of the forebody surface, which could possibly alter the vortex behavior. Therefore, results of the four-strake x case could not be observed.

Test Conditions

The wind tunnel used for the experiments at the Naval Postgraduate School has a test section measuring 28 × 45 in., with a contraction ratio of approximately 10. The ambient turbulence intensity in the wind tunnel is 0.2%. Available speeds were limited by those achievable with turbulence-generating grids used in a related test. The Reynolds number, based on model diameter and freestream velocity, was 1.15×10^5. This particular Reynolds number lies in the laminar Reynolds number range[4]; in the current experiment, then, one might expect the separation characteristics to be similar for both sides of the missile body. No surface flow studies were performed to confirm this expectation.

Obviously, full-scale Reynolds numbers cannot be matched. Yet due to the fact that large side forces have been found to exist in the fully laminar and fully turbulent separation regimes,[7,10] the results may nevertheless be pertinent. As noted by Hall[11] using the data of Keener[4] and Lamont,[7] the Reynolds number can have a significant influence on the development of sectional side force along the body; but the different pressure distributions result in similar overall maximum side forces, as noted by Lamont[7] at Reynolds numbers of 2.0×10^5 and 4.0×10^6.

A conclusion of past tests is that the maximum vortex-induced side force remains fairly constant up to a crossflow Mach number of about 0.4.[3] The envelope of maximum values of C_Y then decreases for increasing subsonic Mach number. A typical flight Mach number for the missile push-over maneuver is about 0.5. The experiments should provide a bound for a possible vortex-induced yawing moment tending to cause the missile to depart.

Results

Nose Roll Angle

The behavior of the nose-generated vortical flow has been found by numerous investigators to be extremely sensitive to the nose roll angle. Apparently, microasymmetries in the ogive-nose geometry are sufficient to influence the direction of the resulting side force, as well as its magnitude, over the range of angles of attack. An angle-of-attack sweep at 5-deg increments was made for nose roll angles at 45-deg increments. For these cases, the wingless body was fixed, while the nose was rotated through the roll-angle variation. Such a procedure eliminated any effect due to body roll angle. The nose-roll angles were referenced to an arbitrary starting point. One nose roll angle resulted in the highest value of C_Y of 3.6 at α = 50 deg. This nose roll angle was maintained for all subsequent tests.

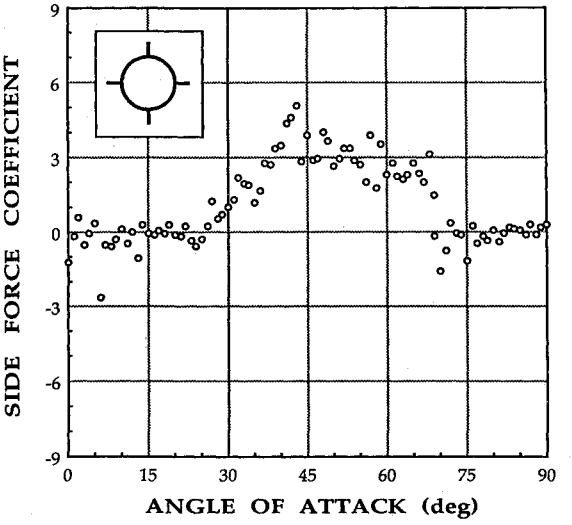

Fig. 4 Side force coefficient, no forebody strakes, + wing afterbody; $Re = 115{,}000$, $M = 0.11$.

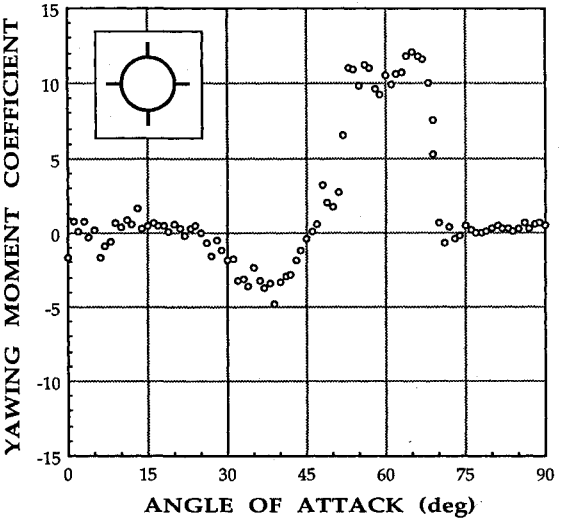

Fig. 5 Yawing moment coefficient, no forebody strakes, + wing afterbody; $Re = 115{,}000$, $M = 0.11$.

Baseline Runs

The nose roll angle was fixed for the tests without forebody strakes, and the body was rotated for the + and x configurations. Resultant side-force and yawing-moment coefficients are shown in Figs. 4–7.

It can be seen in Fig. 4 that induced side forces begin at about α = 25 deg and reach a maximum value of about 5.1 between 40- and 45-deg angle of attack. The yawing moment coefficient curve in Fig. 5 indicates the same range over which there is an induced effect, though a significant difference is seen that will be pointed out in later results as well. Between 25- and 45-deg angle of attack, the yawing moment is negative; there is a switching of sign as the induced moment passes through zero at 45 deg. The values of C_n steeply reach a maximum of over 12 at α = 65 deg. These two figures indicate that the presentation of side-force data alone may fail to relate the important effects of the asymmetric-vortex flowfield; the side force maximizes at an angle of attack where the induced yawing moment is practically zero. More will be said on this presently.

It can be noted in these figures, as in some later figures, that a wide scatter of data exists in C_Y and C_n at angles of attack less than 15 deg. The balance used for the experiments was rated much higher than necessary for these tests; measured forces were in the lowest 10% of the balance span. It is believed that the scatter at low angles where the balance is

relatively unloaded is due to the inherent limitations of the balance accuracy. At angles of attack above 15 deg, the normal force apparently is sufficient to provide the stability needed for the measurement of small side forces. It should be noted that static loadings with small weights performed before each wind-tunnel test did not show this scatter. No other explanation of the phenomenon can be given, and it is believed that the scatter at low angles is due to balance limitations, rather than to measured forces. In no case did the balance show a similar occurrence as zero side forces were reached near 90 deg.

The next two figures show side force and yawing moment coefficients for the x configuration. In this case, the side force values are negative at low angles of attack and become positive between 40 and 45 deg, maximizing at 65 deg. Again, the scatter seen below 15 deg is believed to be due to the causes mentioned above. The yawing moments, on the other hand, initially are positive and become negative briefly between 40 and 45 deg. Betwen 50 and 55 deg the side forces and yawing moments are of identical sign, and peak at the same angle of attack.

The baseline runs indicate a general behavior noted by other investigators but perhaps not sufficiently characterized for a realistic missile configuration. On sharp, slender, axisymmetric forebodies, asymmetric vortex shedding generally begins when the angle of attack exceeds the nose apex angle.[12] For the current model, this onset angle would be about 48–50 deg. Yet blunted ogives attached to cylindrical afterbodies result in the formation of side force cells along the afterbody, which may be significant. For blunt noses or those with steep apex angles, the onset angle of attack is driven by the overall body fineness ratio, l/d. Ericsson and Reding[3] present evidence of the onset angle for such a case of about $4.2(d/l)$. For the missile under study, this would give an onset angle for afterbody-generated asymmetric vortices of about 18–20 deg. Even though the nose fineness ratio is large enough (or the apex angle small enough) to promote the generation of strong asymmetric vortices from the forebody at high angles of attack, the body fineness ratio of 13.06 appears large enough to induce significant side forces and yawing moments at lower angles of attack (between 20 and 45 deg). This combination of mechanisms would explain why the side forces presented in Fig. 4 are induced sooner than expected, and why the initial yawing moments are of opposite sign to the side forces. Considering the side forces alone might give the false impression that the expected yawing moments generated below 45-deg angle of attack are derived from forebody vortices. The C_Y and C_n are of identical sign at high angles of attack, indicating the action of nose-generated vortices providing the induced side force; but as shown for the + case, the maximum induced side force actually results in zero yawing moment at 45 deg. The sign switch at 45–50 deg angle of attack corresponds to that onset angle of attack expected for a slender forebody alone. Side force studies alone, therefore, appear insufficient when considering possible control problems for a realistic missile with a long afterbody.

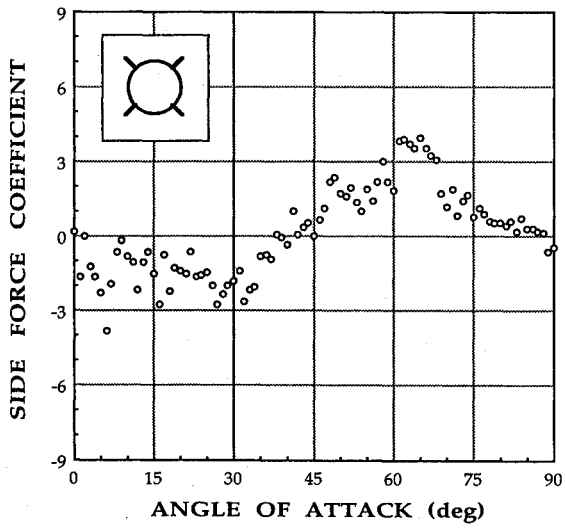

Fig. 6 Side force coefficient, no forebody strakes, x wing afterbody; $Re = 115{,}000$, $M = 0.11$.

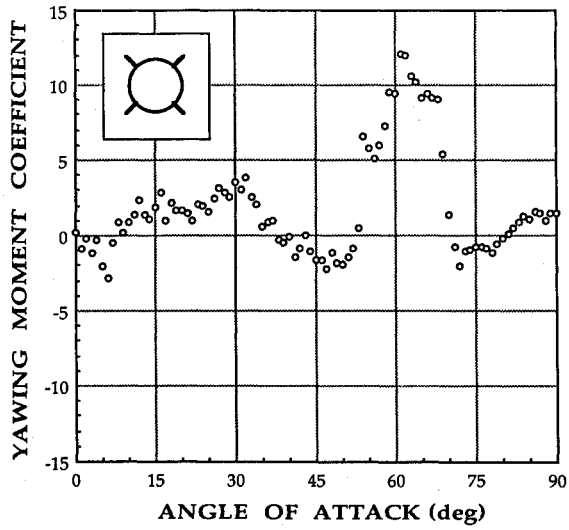

Fig. 7 Yawing moment coefficient, no forebody strakes, x wing afterbody; $Re = 115{,}000$, $M = 0.11$.

Four-Strake Forebody

Four strakes were added to the forebody in the + orientation. The nose roll angle was fixed. Two afterbody configurations were tested.

Figure 8 shows a complete elimination of the induced side forces above 50-deg angle of attack (compared to Fig. 4). The side forces induced over the afterbody from 25–50 deg remain significant and may actually be slightly increased. These results reinforce the previous statement about the forces at low angles of attack being due to afterbody vortices; the strakes have no effect on vortices that detach downstream of the nose region. The flow separates symmetrically at the nose at high angles of attack due to the addition of the strakes; at low angles of attack, asymmetric afterbody vortices form, causing a small but significant side force. The yawing moments in Fig. 9 reflect the same conclusion, with the moments at angles of attack less than 45 deg being undisturbed and those beyond 50

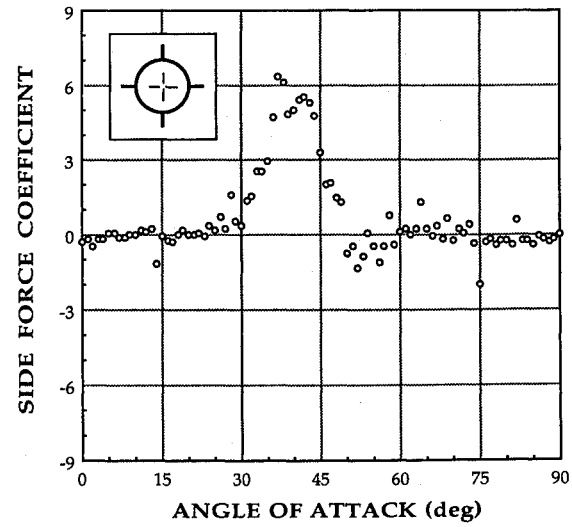

Fig. 8 Side force coefficient, four-strake forebody, + wing afterbody; $Re = 115{,}000$, $M = 0.11$.

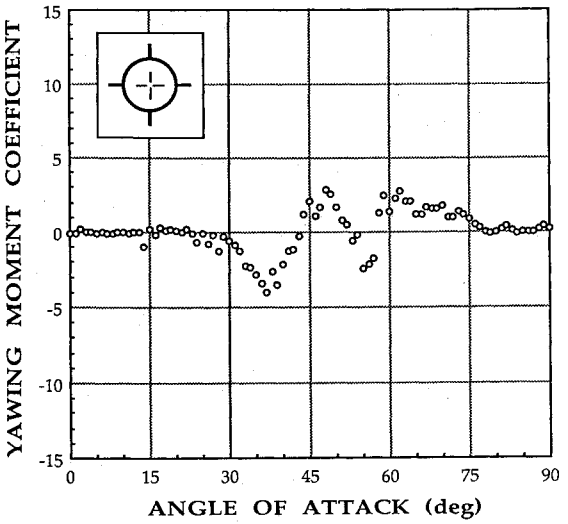

Fig. 9 Yawing moment coefficient, four-strake forebody, + wing afterbody; $Re = 115{,}000$, $M = 0.11$.

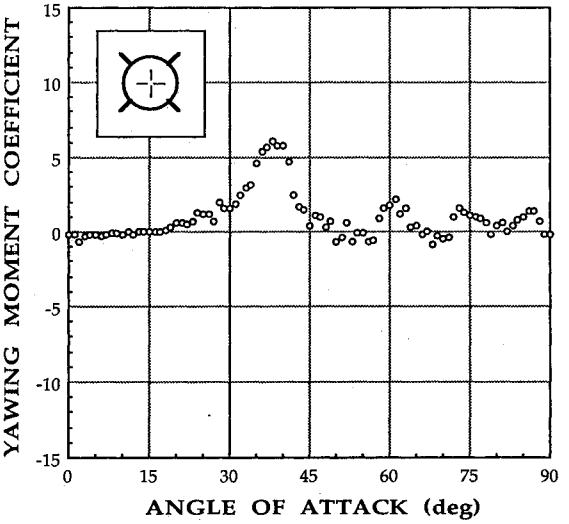

Fig. 11 Yawing moment coefficient, four-strake forebody, x wing afterbody; $Re = 115{,}000$, $M = 0.11$.

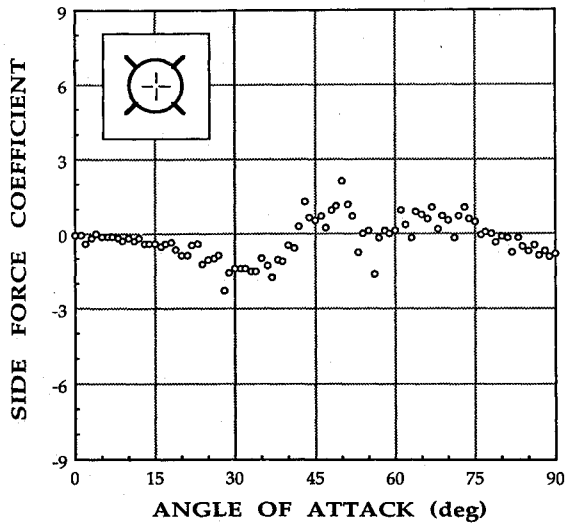

Fig. 10 Side force coefficient, four-strake forebody, x wing afterbody; $Re = 115{,}000$, $M = 0.11$.

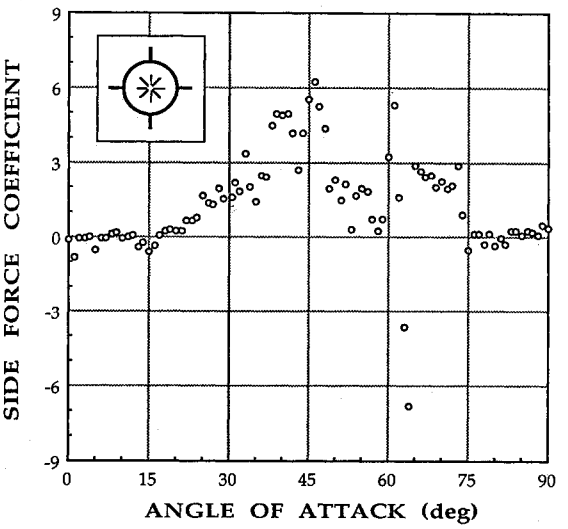

Fig. 12 Side force coefficient, eight-strake forebody, + wing afterbody; $Re = 115{,}000$, $M = 0.11$.

deg being reduced, the maximum value by 75%, from 12 to 3 units. The fixing of the forebody separation location at high angles of attack drives the lee flowfield vortices to remain fairly symmetric. The forces and moments beyond about 45 deg remain of the same sign, indicating the action of weakly-asymmetric forebody vortices beyond 45 deg and afterbody vortices at angles of attack less than 45 deg.

Figures 10 and 11 represent the side-force and yawing-moment coefficients for the x wing configuration. As in the previous case, the four-strake forebody was successful in reducing the induced side forces to a small level at high angles of attack, whereas the values at low angles of attack remained about the same. Comparing Figs. 11 and 7, one sees the yawing moments were likewise practically eliminated in the 50-70 deg angle-of-attack range where a steep peak previously existed. Interestingly, the yawing moments for the low angle-of-attack range from 20 to 45 deg were not only not eliminated but were slightly increased, as noted also for the + case. At low angles of attack, one does not expect nose-generated vortices to form; with the addition of sharp forebody strakes, the flow separates from the forebody strakes at these low angles of attack. Perhaps these vortices generated from the strakes at low angles of attack feed energy into the afterbody vortices, causing an slight enhancement of the yawing moment. The values of C_n are still well below the previous maximum values that were eliminated.

Eight-Strake Forebody

The forebody, placed at the same roll angle as before, was further modified by the addition of four more strakes, resulting in a total of eight strakes, one located every 45 deg radially around the forebody. A sketch and photo of the eight-strake forebody are shown in Fig. 3c. The results of testing this condition for the two body-wing configurations are shown in Figs. 12–15.

The + case is treated in Figs. 12 and 13. The side force response for the eight-strake configuration is somewhat mixed. As before with the four-strake configuration, the induced side forces at low angles of attack remain relatively unchanged. There is a slight reduction in the values beyond 45 deg, but not to the magnitude experienced with the four-strake configuration. Between 60 and 65 deg there is an excursion of values from 5 to −7; a reversal or switching may be taking place, being triggered by the family of vortices being shed from the eight-strake forebody. Such a switching phenomenon has been observed by other investigators.[13,14] Induced side force values remain at levels identical to the baseline case for angles of attack between 65 and 75 deg.

Figure 13 shows the result of the eight-strake forebody on the yawing moment. The afterbody-generated vortices are left unchanged as before; the significant increase in C_n seen in the baseline case has been eliminated between 45 and 60 deg. However, the yawing moments reach high values identical to

those of the baseline case between 65 and 75 deg. Though the range of angle of attack for induced moments has been shortened, it has not been eliminated with this forebody. Apparently the addition of multiple strakes must be done with caution.

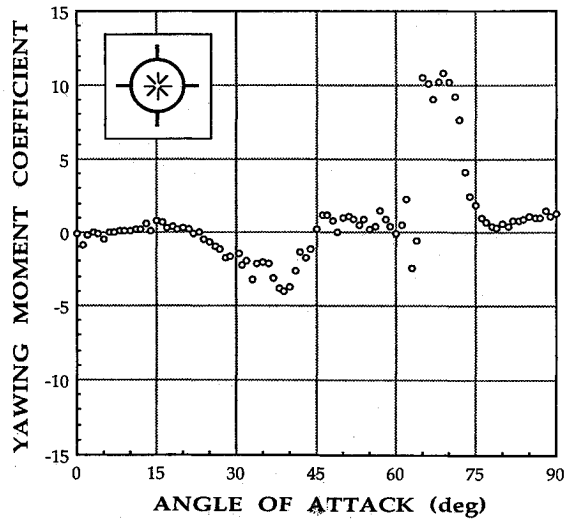

Fig. 13 Yawing moment coefficient, eight-strake forebody, + wing afterbody; $Re = 115{,}000$, $M = 0.11$.

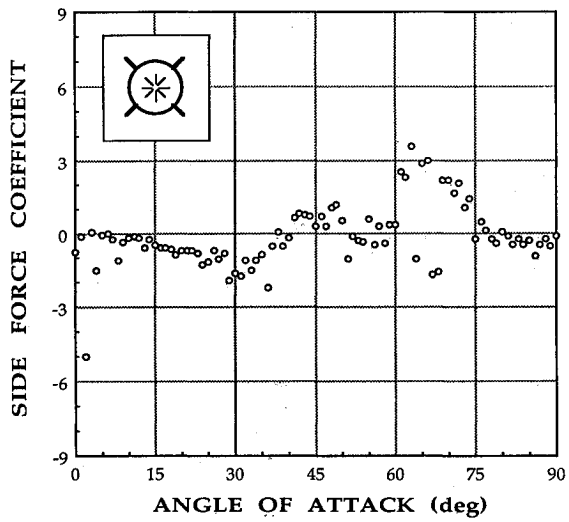

Fig. 14 Side force coefficient, eight-strake forebody, x wing afterbody; $Re = 115{,}000$, $M = 0.11$.

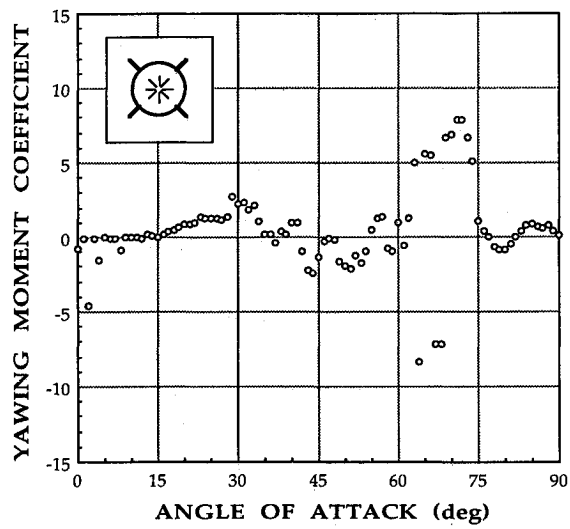

Fig. 15 Yawing moment coefficient, eight-strake forebody, x wing afterbody; $Re = 115{,}000$, $M = 0.11$.

Figures 14 and 15 treat the x configuration. The side forces below 45 deg are relatively undisturbed; very similar to the previous case, the values are reduced between 45 and 60 deg but are maintained at high values between 60- and 75-deg angle of attack. Some switching can be noted between 60 and 70 deg. The yawing moments follow the same pattern. The afterbody-generated values below 45 deg are left undisturbed; from 50 to 60 deg, the yawing moment is eliminated; but between 60 and 75 deg, the moments are only slightly reduced. The same switching can be noted in this region.

Conclusions

The following statements summarize the conclusions reached as a result of the experimental measurements.

1) The onset angle of attack for the formation of asymmetric vortices for this realistically configured missile was driven by the body-length-to-diameter ratio, not by the apex angle of the ogive forebody. The onset angle correlated favorably with previous studies of the onset angle for blunted slender forebodies with long afterbodies.

2) Because of the generation of significant forebody and afterbody vortices, which give yawing moments of opposite sign over the missile, the consideration of induced side forces alone appears insufficient to reveal potential control problems over the angle-of-attack range from 20 to 70 deg. In one case, the angle of attack for maximum side force corresponded to a zero yawing moment.

3) Forebody modifications failed to successfully decrease the induced yawing moments at low angles of attack; this result is due to the fact that these asymmetric vortices are being generated over the afterbody. All afterbody-generated yawing moments had smaller magnitudes than the forebody-generated yawing moments for the baseline forebody, however. The afterbody-induced yawing moments were actually increased slightly in magnitude due to the action of the strakes. A study of the interaction mechanism of the strake vortices with the afterbody vortices is beyond the scope of the present analysis.

4) The four-strake configuration virtually eliminated the induced side forces and yawing moments at angles of attack beyond 50 deg. Forebody vortices may continue to exist, but yawing moments remain small. Apparently the + strake configuration successfully drove the forebody-generated vortices to be symmetric, or nearly so.

5) The effect of the eight-strake forebody configuration was extremely angle-of-attack dependent. Below 45 deg, where the vortices are being generated by the afterbody, no effect was seen, identical to the four-strake case. Between 45 and 60 deg, where the yawing moment greatly increased for the baseline missile, the yawing moments were more or less eliminated. From 60 to 65 deg, an unusual switching or reversal, noted for both body orientations, took place. Beyond 65 deg the yawing moment quickly reached a maximum similar to that for the baseline forebody, and the eight-strake forebody became ineffective. Why this is so is unclear. Evidently, more work needs to be done with the use of multiple strakes, an issue that becomes apparent from a study of the results of Ref. 6 mentioned previously.

6) The wing-body orientation did not significantly influence the effects of the straked forebodies. A previous study had found that the lee flowfield for the two wing-body configurations, even for such low-aspect-ratio wings, can be quite different.[15]

Acknowledgments

The first author would like to thank the Republic of China Navy General Headquarters for providing the opportunity to study in the United States. The authors wish to thank modelmaker John Moulton for construction of the new forebody and strakes. The authors also wish to thank the reviewers and the associate editor for their helpful comments, criticisms, and suggestions.

References

[1]Friedman, N., "Naval Vertical Launch Missile Systems," *Military Technology*, Vol. 9, No. 5, 1985, pp. 24–31.

[2]Gregoriou, G., and Knoche, H.-G., "High Incidence Aerodynamics of Missiles During Launch Phase," Messerschmitt-Bolkow-Blohm GmbH, Ottobrunn/Munich, Germany, UA-523/80, Jan. 1980.

[3]Ericsson, L. E., and Reding, J. P., "Asymmetric Vortex Shedding from Bodies of Revolution," *Tactical Missile Aerodynamics*, Vol. 104, *Progress in Astronautics and Aeronautics*, edited by M. J. Hemsch and J. N. Nielsen, AIAA, New York, 1986, pp. 243–296.

[4]Keener, E. R. , "Flow-Separation Patterns on Symmetric Forebodies," NASA TM-86016, Jan. 1986.

[5]Yongnian, Y., Xinzhi, Y., and Jianying, L., "Active Control of Asymmetric Forces at High Incidence," *Journal of Aircraft*, Vol. 25, No. 2, 1988, pp. 190–192.

[6]Dunne, A. L., Black, S., Schmidt, G. S., and Lewis, T. L., "VLA Missile Development and High Angle of Attack Behavior," *Proceedings of NEAR Conference on Missile Aerodynamics*, edited by M. R. Mendenhall, D. Nixon, and M.F.E. Dillenius, NEAR, Inc., Mountain View, CA, 1988, pp. 13-1–13-68.

[7]Lamont, P. J., "Pressures Around an Inclined Ogive Cylinder with Laminar, Transitional, or Turbulent Separation," *AIAA Journal*, Vol. 20, No. 11, 1982, pp. 1492–1499.

[8]Lamont, P. J., "The Complex Asymmetric Flow Over a 3.5D Ogive Nose and Cylindrical Afterbody at High Angles of Attack," AIAA Paper 82-0053, Jan. 1982.

[9]Howard, R. M., Rabang, M. P., and Roane, D. P., Jr., "Aerodynamic Effects of a Turbulent Flowfield on a Vertically-Launched Missile," *Journal of Spacecraft and Rockets*, Vol. 26, No. 6, 1989, pp. 445–451.

[10]Champigny, P., "Reynolds Number Effect on the Aerodynamic Characteristics of an Ogive-Cylinder at High Angles of Attack," AIAA Paper 84-2176, Aug. 1984.

[11]Hall, R. M., "Influence of Reynolds Number on Forebody Side Forces for 3.5-Diameter Tangent-Ogive Bodies," AIAA Paper 87-2274, Aug. 1987.

[12]Keener, E. R., and Chapman, G. T., "Onset of Aerodynamic Side Forces at Zero Sideslip on Symmetric Forebodies at High Angles of Attack," AIAA Paper 74-770, Aug. 1974.

[13]Clark, W. C., and Nelson, R. C., "Body Vortex Formation on Missiles at High Angles of Attack," AIAA Paper 76-65, Jan. 1976.

[14]Deffenbaugh, F. D., and Koerner, W. G., "Asymmetric Vortex Wake Development on Missiles at High Angles of Attack," *Journal of Spacecraft and Rockets*, Vol. 14, No. 2, 1977, pp. 155–162.

[15]Howard, R. M., Lung, M.-H., Viniotis, J. J., Johnson, D. A., and Pinaire, J. A., "Wing Effects on Asymmetric Vortex Formation for a Ship-Launched Missile," AIAA Paper 90-2851, Aug. 1990.

Ernest V. Zoby
Associate Editor